



A strong parietal hub in the *small-world* network of coloured-hearing synaesthetes during resting state EEG

Lutz Jäncke* and Nicolas Langer

Division Neuropsychology, Psychological Institute, University of Zurich, Switzerland

We investigated whether functional brain networks are different in coloured-hearing synaesthetes compared with non-synaesthetes. Based on resting state electroencephalographic (EEG) activity, graph-theoretical analysis was applied to functional connectivity data obtained from different frequency bands (theta, alpha1, alpha2, and beta) of 12 coloured-hearing synaesthetes and 13 non-synaesthetes. The analysis of functional connectivity was based on estimated intra-cerebral sources of brain activation using standardized low-resolution electrical tomography. These intra-cerebral sources of brain activity were subjected to graph-theoretical analysis yielding measures representing small-world network characteristics (cluster coefficients and path length). In addition, brain regions with strong interconnections were identified (so-called hubs), and the interconnectedness of these hubs were quantified using degree as a measure of connectedness. Our analysis was guided by the two-stage model proposed by Hubbard and Ramachandran (2005). In this model, the parietal lobe is thought to play a pivotal role in binding together the synaesthetic perceptions (hyperbinding). In addition, we hypothesized that the auditory cortex and the fusiform gyrus would qualify as strong hubs in synaesthetes. Although synaesthetes and non-synaesthetes demonstrated a similar small-world network topology, the parietal lobe turned out to be a stronger hub in synaesthetes than in non-synaesthetes supporting the two-stage model. The auditory cortex was also identified as a strong hub in these coloured-hearing synaesthetes (for the alpha2 band). Thus, our *a priori* hypotheses receive strong support. Several additional hubs (for which no *a priori* hypothesis has been formulated) were found to be different in terms of the degree measure in synaesthetes, with synaesthetes demonstrating stronger degree measures indicating stronger interconnectedness. These hubs were found in brain areas known to be involved in controlling memory processes (alpha1: hippocampus and retrosplenial area), executive functions (alpha1 and alpha2: ventrolateral prefrontal cortex; theta: inferior frontal cortex), and the generation of perceptions (theta: extrastriate cortex; beta: subcentral area). Taken together this graph-theoretical analysis of the resting state EEG supports the two-stage model in demonstrating that the left-sided parietal lobe is a strong hub region, which is stronger functionally interconnected in synaesthetes than in non-synaesthetes. The

*Correspondence should be addressed to Lutz Jäncke, Division Neuropsychology, Binzmühlestrasse 14, 8050 Zurich, Switzerland (e-mail: ljaencke@psychologie.uzh.ch).

right-sided auditory cortex is also a strong hub supporting the idea that coloured-hearing synaesthetes demonstrate a specific auditory cortex. A further important point is that these hub regions are even differently operating at rest supporting the idea that these hub characteristics are predetermining factors of coloured-hearing synaesthesia.

Synaesthesia is a psychological phenomenon that has attracted increasing scientific interest (Mattingley, 2009). In synaesthesia, stimulation of one sensory modality results in additional precepts being evoked simultaneously and automatically (Cytowic & Wood, 1982a,b; Hubbard & Ramachandran, 2005). The most frequent form of synaesthesia is grapheme-colour synaesthesia in which a particular grapheme (the inducer) elicits a particular colour perception (the concurrent perception) (Simner, 2007). Other than this frequently occurring form of synaesthesia, several other variants have been reported, including coloured-hearing (Goller *et al.*, 2009), music-taste (Beeli *et al.*, 2005), colour-people (Weiss, Shah, Toni, Zilles, & Fink, 2001), sound-touch (Beauchamp & Ro, 2008), ordinal linguistic personification (Simner & Hoenstein, 2007), word-taste (Simner & Ward, 2006), mirror-touch synaesthesia (Banissy & Ward, 2007), as well as other variants of synaesthesia (see Mattingley, 2009, for a summary). Traditional definitions emphasize that synaesthesia is unidirectional. This means that the inducer always induces the concurrent perception but the concurrent perception does not have the potential to act as the inducer. An instance of this would be when the grapheme /a/ evokes the colour red but red does not induce the perception of an /a/. Nonetheless, this notion is currently challenged due to several studies that have demonstrated bidirectional (at least implicit) forms of synaesthesia (Brang, Edwards, Ramachandran, & Coulson, 2008, 2010; Meier & Rothen, 2007, 2009; Rothen, Nyffeler, von Wartburg, Müri, & Meier, 2010; Weiss, Kalckert, & Fink, 2009).

The origins of synaesthesia are not entirely understood. Currently, genetic- and experience-dependent influences are being discussed (Barnett *et al.*, 2008; Beeli, Esslen, & Jäncke, 2007). In addition, the neurophysiological and neuroanatomical underpinnings of the different variants of synaesthesia are currently unknown. Hubbard and Ramachandran (2005, 2007) and Hubbard, Brang, and Ramachandran (2011) integrated several findings and proposed a two-stage model of grapheme-colour synaesthesia with cross-activation between aberrantly connected brain regions and hyperbinding of two perceptions. According to this model, cross-activation occurs because of an abnormal excess of connections between the grapheme and colour processing brain areas. Due to this aberrant connection, the involved areas are strongly coactivated during grapheme and/or colour processing. The second stage entails both perceptions being bound together by parietal mechanisms, resulting in hyperbinding. In particular, the parietal cortex (especially the intraparietal sulcus and/or superior parts of the parietal lobe) is thought to be essentially involved in hyperbinding. In synaesthetes, this area should be strongly activated or better connected with other brain regions involved in synaesthesia. Cross-activation is thought to be responsible for the particular kind of synaesthesia. For example, grapheme-colour synaesthetes should have an aberrantly strong cross-activation between the grapheme and colour areas in the posterior inferior temporal cortex region (with the fusiform gyrus as the main landmark region).

Several brain-imaging studies have provided support for this model, at least for grapheme-colour synaesthesia (Beeli, Esslen, & Jäncke, 2008; Cohen Kadosh, Cohen Kadosh, & Henik, 2007; Esterman, Verstynen, Ivry, & Robertson, 2006; Muggleton, Tsakanikos, Walsh, & Ward, 2007; Rouw & Scholte, 2007, 2010; Weiss, Zilles, & Fink, 2005). By employing measures of fractional anisotropy (FA) and grey matter density

in grapheme-colour synaesthetes, specific anatomical features have been identified that are also in the vicinity of the parietal cortex of synaesthetes (Rouw & Scholte, 2007, 2010; Rouw, Scholte, & Colizoli, 2011; Weiss *et al.*, 2005).

Whether this model holds true for other forms of synaesthesia (e.g., coloured-hearing as examined in our study) has yet to be demonstrated. For coloured-hearing synaesthetes, cross-activation should occur between the auditory cortex and the colour area within the fusiform cortex. The distance between both areas is relatively long; nevertheless, it has been shown that both areas are simultaneously activated when coloured-hearing synaesthetes hear letters or digits (Beeli *et al.*, 2008). Hyperbinding is considered to operate independently from this particular type of synaesthesia. Thus, the parietal cortex (and particularly the intraparietal sulcus) should also be specific in coloured-hearing synaesthetes.

Cross-activation and *hyperbinding* are two processes that abnormally utilize the interconnectedness and functional connectivity of the human brain. Functional coupling of adjacently and distally located brain areas is a unique phenomenon of the human brain, which is not only present during the processing of more or less demanding tasks; it is present even during rest (Jann *et al.*, 2009; Jann, Koenig, Dierks, Boesch, & Federspiel, 2010; Laufs, 2008; Laufs *et al.*, 2003a, b). Nevertheless, there is currently no study available, which has explicitly demonstrated different connectivity patterns in synaesthetes. Therefore, we designed this study, in order to examine whether synaesthetes (here coloured-hearing synaesthetes) demonstrate different functional connectivity patterns.

Several recent studies have demonstrated that functional brain connections are organized in a highly efficient *small-world* manner (Bullmore & Sporns, 2009; Sporns, Chialvo, Kaiser, & Hilgetag, 2004; Sporns, Honey, & Kötter, 2007; Stam, 2004; Stam, 2010). To mathematically describe *small-world* networks, graph-theoretical analysis techniques are generally used (Bullmore & Sporns, 2009). These are abstract representations of networks, consisting of sets of vertices (nodes) linked by edges (connections). A *cluster coefficient* (C) and a characteristic *path length* (L) are the typical parameters describing the properties of *small-world* networks. Compared with a random network, a high C and a low L characterize *small-world* networks. A high C and a low L suggests that a high level of local neighbourhood clustering (as indexed by C) is responsible for efficient local information processing in conjunction with several long-distance connections (indexed by L) that ensure a high level of global communication efficiency across the network and integration of information between the different regions of the brain (Bullmore & Sporns, 2009). A further important measure of small-world networks is *centrality* (or *degree*), which indicates how strongly a particular hub is interconnected with the *small-world* network.

Network analyses have been applied to patterns of functional connectivity patterns during the resting state, as measured with EEG, magnetoencephalography (MEG), and functional magnetic resonance imaging (fMRI) in order to explore inter-individual differences concerning the *small-world* characteristics. For example, the *small-world* networks of Alzheimer's patients are disrupted or diminished, mostly in the direction of a more random network organization (Bartolomei *et al.*, 2006; Li *et al.*, 2009; Micheloyannis *et al.*, 2006, 2009; Ponten, Daffertshofer, Hillebrand, & Stam, 2010; Rubinov *et al.*, 2009; Stam, Jones, Nolte, Breakspear, & Scheltens, 2007). In addition, psychometric intelligence is related to particular *small-world* network characteristics (van den Heuvel, Stam, Kahn, & Hulshoff Pol, 2009).

In the present study, we readdress the issue whether *small-world* network characteristics are related to inter-individual differences in cognition. Here, we examine whether coloured-hearing synaesthetes demonstrate different *small-world* network characteristics compared with non-synaesthetes by using resting state EEG in association with a valid method, to estimate the intra-cerebral sources of surface EEG (standardized low-resolution electrical tomography [sLORETA]) (Pascual-Marqui, 2002). Based on the two-stage model proposed by Hubbard (2007), we hypothesize that synaesthetes should have a strong network hub in the parietal lobule subserving *hyperbinding* and other strong hubs in the fusiform gyrus (processing colour) and the auditory cortex (processing tones). We are particularly interested in the interconnectedness of these hubs, which can be expressed in specific measures proposed by the graph-theoretical analysis. In this study, we will use degree as a particular measure of local interconnectedness. Therefore, this measure should be stronger for coloured-hearing synaesthetes in the hypothesized regions.

In this study, we focus on the so-called resting EEG and its relation to coloured-hearing synaesthesia. Resting EEG is the tonic EEG activation pattern of subjects in a relaxed state during that they are not executing a particular psychological task. The intra-individual stability of resting EEG measures has been demonstrated repeatedly for different frequency bands (Näpflin, Wildi, & Sarnthein, 2007). In addition, resting EEG is strongly determined by genetic factors (Ambrosius *et al.*, 2008; Anokhin, Lutzenberger, & Birbaumer, 1999; Ivonin, Tsitseroshin, Pogosyan, & Shuvaev, 2004; Linkenkaer-Hansen *et al.*, 2007; Orekhova, Stroganova, Posikera, & Malykh, 2003; Posthuma, Neale, Boomsma, & de Geus, 2001; Smit, Wright, Hansell, Geffen, & Martin, 2006; Tang *et al.*, 2007). Thus, resting EEG can be taken as a stable biological marker for individual brain activity.

Methods

Subjects

The analysis and this paper are based on the data obtained in the context of a study published in Beeli *et al.* (2008). Thus, we will only shortly describe the included subjects and the methods to confirm the presence of synaesthesia. In this study, we report data from 12 synaesthetes and 13 non-synaesthetes matched for sex, education, and age (mean age \pm standard deviation: synaesthetes 25.7 ± 9.1 , controls 26.1 ± 6.4 ; mean years of education: synaesthetes 15.3 ± 1.8 , controls 14.3 ± 0.9 ; groups did not differ significantly: $p = .88$ for age, and $p = .13$ for education). All synaesthetes reported lifelong history of 'color-hearing' synaesthesia and they were tested for their colour perception to letters (A-Z) and numbers (0-9). They were asked to produce their synaesthetic colours elicited by auditorily presented letters and digits as accurately as possible using a digital image-editing software (Adobe Photoshop 7.0). All synaesthetes had to repeat this task (on average 55 days later), and all of them demonstrated constant and consistent reproduction. None of the synaesthetes reported to experience additional synaesthetic experiences over and above the reported and verified coloured-hearing synaesthesia.

EEG recording and processing

Resting EEG was recorded using a 30 channel EEG montage according to the 10-10 system (Fp1/2, F3/4, F7/8, Fz, FT7/8, FC3/4, FCz, T7/8, C3/4, Cz, TP7/8, CP3/4, CPz, P7/8, P3/4, Pz, O1/2, Oz) with the BrainAmp system of BrainProducts, Munich, Germany.

In addition, two EOG channels were corecorded, located below the left and right outer canthi of the eyes. Recording reference was at FCz, with off-line re-referencing to average reference. Digital sampling rate was 500 Hz, on-line filtering 0.1–100 Hz, off-line filtering 0.5–30 Hz, impedance was kept below 10k ohm.

For measuring resting EEG subjects were required to sit comfortably in a chair in a dimly illuminated, sound-shielded Faraday recording cage. Subjects were instructed that EEG recording is done while they rested with their eyes repeatedly open or closed. The EEG protocol consisted of the participants resting with their eyes open for 20 s, followed by 40 s with their eyes closed; this was repeated three times. Only data from the 120 s eyes closed condition were analysed. After the recording of the resting EEG, subjects participated in an event related potential (ERP) experiment, which has been reported elsewhere (Beeli *et al.*, 2008).

For EEG analysis, the data were segmented into 2 s windows. In a second step, a discrete Fourier transformation algorithm was applied to all artefact-free 2 s epochs (45 segments per subjects). The power spectrum of 1.5–30 Hz (resolution: 0.488 Hz) was calculated. The spectra for each channel were averaged over all epochs for each subject. Absolute power spectra were integrated for the following five independent frequency bands following classification proposed by Kubicki, Herrmann, Fichte, and Freund (1979): theta (6.5–8 Hz), alpha1 (8.5–10 Hz), alpha2 (10.5–12 Hz), beta (12.5–21 Hz). We know that the theta band is defined in some studies with a broader range (e.g., 4–8 Hz) (Kahana, Sekuler, Caplan, Kirschen, & Madsen, 1999; Klimesch, 1999; Tesche & Karhu, 2000). However, we decided to use the slightly smaller band range because this is provided by the sLORETA software and is frequently used in recent publication (Gianotti *et al.*, 2009; Jausovec & Jausovec, 2000; Kubicki *et al.*, 1979).

Scalp map analysis (topographical map analysis)

After the preprocessing steps, the data of 30 electrodes were compared between synaesthetes and non-synaesthetes for each frequency band. The topographical plots of power values and the associated differences were inspected for between-group differences.

Source localization

For the purpose of estimating the intra-cerebral electrical sources that generated the scalp-recorded activity, sLORETA, (Pascual-Marqui, 2002) was employed (freely available at <http://www.uzh.ch/keyinst/loreta.htm>). The following description of the used LORETA method is taken from the description provided by the author of LORETA and published on his website <http://www.uzh.ch/keyinst/NewLORETA/Methods/MethodsEloreta.htm>. The author explicitly encourages researchers to use his formulation for describing the LORETA technique. sLORETA computes, from the recorded scalp electric potential differences, the three-dimensional (3D) distribution of the electrically active neuronal generators in the brain as standardized units of current density (A/cm^2) at each voxel by assuming similar activation among neighbouring neuronal clusters (Pascual-Marqui, 2002). In the current implementation of sLORETA, computations were made in a realistic head model (Fuchs, Kastner, Wagner, Hawes, & Ebersole, 2002), using the MNI152 template (Mazziotta *et al.*, 2001), with the 3D solution space restricted to cortical grey matter, as determined by the probabilistic Talairach atlas (Lancaster *et al.*, 2000). The standard electrode positions on the MNI152 scalp were taken from Jurcak, Tsuzuki, and Dan (2007) and Oostenveld and Praamstra (2001). The intra-cerebral volume is partitioned in 6,239 voxels at 5-mm spatial resolution. Thus, sLORETA

images represent the standardized electric activity expressed as the exact magnitude of the estimated current density at each voxel in the MNI space (Montreal Neurological Institute). Anatomical labels (as Brodmann areas) are also reported using MNI space, with correction to Talairach space (Brett, Johnsrude, & Owen, 2002). sLORETA ‘solves’ the inverse problem by taking into account the well-known effects of the head as a volume conductor. Conventional LORETA and the more recent sLORETA analyses have been frequently used in previous experiments to localize brain activations on the basis of EEG or MEG data (Langer, Beeli, & Jäncke, 2010; Meyer, Baumann, & Jäncke, 2006; Mulert *et al.*, 2004; Zaehle *et al.*, 2009).

Graph-theoretical network analysis

A graph-theoretical network analysis was conducted to analyse connectivity parameters for the intra-cerebral brain oscillations on the basis of the intra-cerebral oscillations. Several studies conclude that an intra-cortical approach represents a clear methodological improvement compared to the EEG spectral analysis at surface electrodes (Babiloni *et al.*, 2004; Lehmann, Faber, Gianotti, Kochi, & Pascual-Marqui, 2006; Mulert *et al.*, 2004; Sinai & Pratt, 2003). Two-second epochs of EEG-data of each subject were imported into the sLORETA software. Within the sLORETA analysis framework, coherence between 84 anatomical regions of interest (ROI) in both hemispheres was computed. Coherence was calculated as linear instantaneous connectivity. This measure was used in other studies before (De Vico Fallani *et al.*, 2010) and is deemed an adequate measure for computing resting state networks. Linear instantaneous connectivity is a function that operates in the frequency domain and generates a value between 0 and 1. Given two signals x and y , the linear instantaneous connectivity is calculated in a particular frequency f by taking the square of the cross-spectrum

$$|S_{xy}(f)|^2$$

and the dividing by the product of the two corresponding auto power spectra:

$$SC_{xy}(f) = \frac{|S_{xy}(f)|^2}{S_{xx}(f)S_{yy}(f)}.$$

In the present study, the linear instantaneous connectivity SC is calculated between the signals of each cortical source ROI. The sLORETA head model, a standardized template in MNI space including cortical areas of the brain, was parcellated into 84 Brodmann areas to compute the coherence between the centre voxels of each of the 84 ROI. We chose to use the centroid voxels of each ROI instead of calculation of average coherence measures of each ROI, because sLORETA estimates the solution of the inverse problem based on the assumption that the smoothest of all possible activation distributions is the most plausible one. This assumption is supported by neurophysiological data demonstrating that neighbouring neuronal populations show highly correlated activity (Michel *et al.*, 2009). Because of the assumptions of sLORETA, signals of spatially adjacent voxels of neighbouring ROIs are highly correlated, inducing larger coherence, which might be not physiological in nature. By taking just the single-centre voxel of each ROI, we could exclude such contamination. Because of the spatially smooth inverse solution of sLORETA, information of the centroid voxel is an accurate representative for activity within the ROIs.

Intra-cerebral coherence measures of 84 ROIs were subjected to graph-theoretical network analysis. The input for this analysis consisted of an 84×84 coherence-matrix

of the measures of each ROI (84 ROIs) for each subject. Therefore, for each subject, the fields of the matrix represent the edges of the network (graphs). An individual network G_i is represented by the weighted connectivity matrix with N_j nodes and K_{xy} edges, where nodes represent ROIs and edges represent the undirected weighted connections (correlations) between the signals of ROIs. From the number of edges, the density of the networks was computed, which is calculated as number of observed connections divided by the number of possible connections. Because binary and weighted network analyses revealed almost identical results, we only report the weighted analyses in this paper.

The networks of all subjects were averaged to one mean network. Different correlation thresholds (ranging from 0.55 to 0.95) were applied to the average correlation matrix resulting in graphs that comprise different number of edges (connections). The so obtained thresholded mean connectivity matrices were then subjected to the network analysis software *tnet* (Opsahl, 2009) to quantify *small-worldness* (Bullmore & Sporns, 2009; Watts & Strogatz, 1998). *Small-world* indices were derived from the comparison of the real (measured) networks with 100 randomized network realizations comprising the same number of nodes and edges as the real network (Opsahl, Colizza, Panzarasa, & Ramasco, 2008). From the comparison of measured functional brain networks and similar randomized artificial networks, key characteristics that describe the overall architecture of a network were computed. The following definitions of the key measures and key characteristics of small-world networks have been presented in many previous papers. In our paper we refer to several publications from which we have adapted our descriptions and definitions (Bullmore & Sporns, 2009; Humphries & Gurney, 2008; Humphries, Gurney, & Prescott, 2006; Sporns et al., 2004; van den Heuvel et al., 2009; Verstraete et al., 2011; Watts & Strogatz, 1998): key characteristics of *small-world* networks are the *clustering coefficient* C , the characteristic *path length* L , and the *degree* measures D (analysed in the regional node analysis section) (Watts & Strogatz, 1998). The *clustering coefficient* C is given by the ratio between the number of connections between the direct neighbours of a node and the total number of possible connections between these neighbours and provides information about the level of local connectedness within a network. The characteristic *path length* L of a network gives the average number of connections that have to be crossed to travel from each node to every other node in the network and provides information about the level of global communication efficiency of a network (van den Heuvel et al., 2009).

Small-world organized networks are distinguished by a *clustering coefficient* C that is higher than the C of a comparable randomly organized network (C random), but still with a short characteristic *path length* L that is similar to that of an equivalent random network (L random) (Humphries & Gurney, 2008; Humphries, Gurney, & Prescott, 2006; Watts & Strogatz, 1998). Formally, *small-world* networks show a ratio γ defined as C real/ C random of >1 and a ratio λ defined as L real/ L random of ~ 1 (Humphries & Gurney, 2008; Watts & Strogatz, 1998). A high γ reflects a high level of local neighbourhood clustering within a network, and a short normalized travel distance λ expresses a high level of global communication efficiency within a network (Bullmore & Sporns, 2009; Sporns et al., 2004; Watts & Strogatz, 1998). In other words, a *small-world* organization is a modular configuration, which means, that the brain is organized with different information processing centres and they are connected to each other very effectively.

In a first step, a mean coherence matrix (averaged across all subjects) was thresholded with a set of different thresholds (ranging from 0.55 to 0.95). In a second step, the network parameters (clustering coefficient, path length, γ and λ) were calculated for the different thresholded mean coherence matrices. The threshold, which the mean coherence matrices resembled most to small-world topology were chosen for the

following analyses. This particular threshold (only one for each frequency band) was applied for each individual subject.

Regional node analysis

In order to identify and discriminate important hub regions within the *small-world*, *degree* (D) measures were calculated for each individual node and plotted as *degree distribution* (Freeman, 1978; Opsahl & Panzarasa, 2009). *Degree* (which is a particular *centrality* measure) is defined as the sum of weights incident upon a particular node (i.e., the sum of weights of the edges connected to a particular node). Therefore, every node is characterized by its own *degree* value. To visualize the *degree* values graphically, MATLAB software (MathWorks, 2007) was used.

Statistical analysis

Because of the relative small number of subjects and extremely large number of variables, it is nearly impossible to conduct classical statistical inference test. The reason is the small power even when strong effect sizes are present. Thus, when applying corrections for multiple tests (which is necessary to perform statistical tests with large numbers of variables on the same dataset), no or only a few of the very strong effects would have been identified. Because of this, we decided to use a different more descriptive statistical procedure for most of the statistical tests. For a subset of brain regions, we performed a hypothesis-driven statistical analysis (step 3 mentioned below). For these comparisons, we draw stronger conclusions from the analyses. For hypothesis-free analyses, the statistical test results are not interpreted in terms of statistical significance, they are rather used as descriptive measures of between-group differences. For these analyses, we will be more reluctant in interpreting the findings. The p -values for these between-group comparisons can be taken as measures of effect (steps 1, 2, and 4 mentioned below) (Krauth, 1988). Since we have to consider the fact that p -values depend on sample size, we also calculated effect sizes according to Cohen (1969). A $d > .5$ is considered as being moderate, while a $d > .8$ is considered as being large. We will only comment on effects associated with a $p \leq .05$ or a $d > .8$ (large effect size). For the sake of completeness, d and p values will be reported for all analyses (hypothesis-driven and hypothesis-free). All statistical analyses were performed using PASW statistics 18 for MAC. Our statistical analysis comprised the following steps:

- (1) A topographical analysis was performed comparing coloured-hearing synaesthetes with non-synaesthetes for each frequency band and each electrode. This analysis was deemed important to ensure that no general activation differences exist between coloured-hearing synaesthetes and non-synaesthetes.
- (2) For each frequency band, a between-groups test (synaesthetes vs. control subjects) using t -test for independent samples was performed for the general small-world indices (number of edges, density, clustering coefficient, and path length). Similarly as for step 1, we did not formulate an explicit hypothesis, since there is currently no data available suggesting a general whole-brain difference with respect to the small-world topology in coloured-hearing synaesthetes.
- (3) Based on our explicit hypothesis formulated in the introduction of this paper, we anticipated specific network features in three brain areas, which are hypothesized to be pivotal for coloured-hearing synaesthetes: the parietal cortex, the fusiform gyrus, and the auditory cortex. Since hyperbinding and cross-activation are implicated with synaptic strength and thus the number of connections, the degree measure is

used to quantify the connectedness of these areas with other brain areas. In other words, we anticipate stronger degree measures for the parietal cortex, the fusiform gyrus, and the auditory cortex in coloured-hearing synaesthetes. These areas are denoted as hubs in the language of graph-theorem analysis as performed in this study.

- (4) Brain areas (or hubs), for which no explicit hypotheses were formulated (hypothesis-free analyses) showing degree measures, which are larger in coloured-hearing synaesthetes than in non-synaesthetes (surpassing the criterion of a $d > 0.8$ and a $p \leq .05$), are only shortly mentioned and we will refrain from making too strong arguments. Future studies should concentrate on these findings in more detail especially with larger sample sizes.

Results

Topographical EEG analysis

Using *t*-tests for independent samples, the power in each frequency band was compared between coloured-hearing synaesthetes and non-synaesthetes. There were no between-group differences ($p > .10$ and $d < .8$). Thus, we interpret these findings as indicators of similar topographical EEG activations for synaesthetes and non-synaesthetes.

Graph-theoretical network analysis

For the theta band, the network (the average correlation matrix) with the best *small-world* organization characteristics comprises 84 nodes and 2,354 edges with a density = 0.338. Across the whole range of relevant correlation thresholds, the threshold of $r = .85$ represents the best *small-world* network organization, which is defined by a high γ and a $\lambda \approx 1$. For the alpha1 frequency band the network with the best *small-world* network organization consists 2,028 edges with a density of 0.406 (threshold $r = .9$). The best network of the alpha2 frequency band is found at the threshold $r = .8$. Hence, the *small-world* alpha2 frequency band network composed of 3,044 edges and a density = 0.437. For the beta frequency band the threshold $r = .85$ represents the best *small-world* network organization. The resulting network is based on 3,230 edges with a density = 0.463. Table 1 displays the best *small-world* indices for each frequency band.

After applying these specific thresholds (one threshold for each frequency band) to each subject, the small-world indices (*edges*, *cluster coefficient*, *path length*,

Table 1. Table represents the small-world indices identified for the best small-world network organization of all frequency bands

| Frequency band | Theta | Alpha1 | Alpha2 | Beta |
|---------------------|-------|--------|--------|-------|
| Best threshold | 0.85 | 0.9 | 0.8 | 0.85 |
| Edges | 2354 | 2828 | 3044 | 3230 |
| Density | 0.338 | 0.406 | 0.437 | 0.463 |
| CC weighted | 0.689 | 0.704 | 0.716 | 0.722 |
| Path length | 1.836 | 1.663 | 1.609 | 1.548 |
| Weighted normalized | | | | |
| γ weighted | 1.546 | 1.416 | 1.364 | 1.337 |
| λ weighted | 1.101 | 1.044 | 1.039 | 1.007 |

Table 2. Listed are t - and p -values obtained for the t -tests comparing the synaesthetes and non-synaesthetes with respect to the global small-world indices broken down for each frequency band

| | | Edges | CC weighted | PL norm |
|--------|-------------------|--------|-------------|---------|
| Theta | t ($df = 23$) | -1.265 | -0.15 | 1.282 |
| | p | .219 | .882 | 0.214 |
| Alpha1 | t ($df = 23$) | -1.154 | 0.396 | 0.669 |
| | p | .26 | .697 | 0.51 |
| Alpha2 | t ($df = 23$) | 0.749 | 1.078 | -0.286 |
| | p | .462 | .292 | 0.778 |
| Beta | t ($df = 23$) | 0.232 | 0.735 | -0.057 |
| | p | .819 | .47 | 0.955 |

degree) were calculated for each subject individually. The graph-theoretical network analysis for the global *small-world* indices revealed no between-groups differences. All between-group analyses are summarized in Table 2. As one can see from Table 2, all p values are $<.05$.

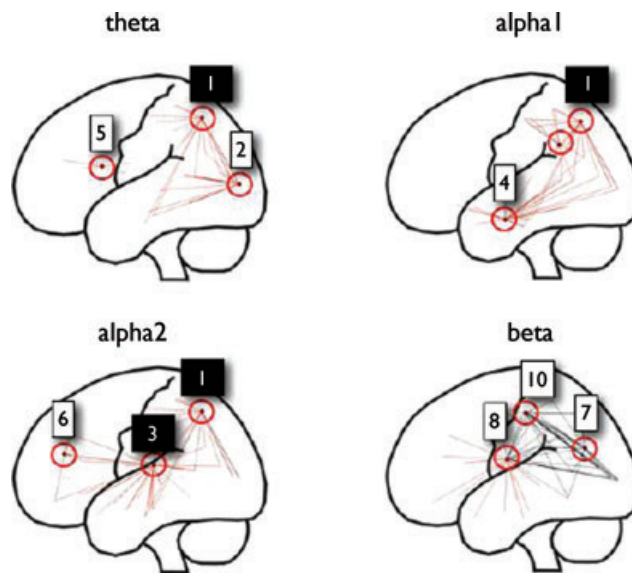


Figure 1. Indicated are the *hubs* for which synaesthetes demonstrate larger *degree* measures (1: parietal lobe; 2: extrastriate cortex; 3: auditory cortex; 4: hippocampus; 5: inferior frontal cortex; 6: ventrolateral prefrontal cortex (anterior portion); 7: angular gyrus; 8: subcentral area; 9: retrosplenial area; 10: postcentral gyrus). Those hubs for which *a priori* hypotheses are present are indicated as black rectangles with digits in white. Please note that one parietal hub for the beta band is located more anteriorly and inferiorly (postcentral gyrus) than the hubs for the other frequency bands. The other hub found in the parietal lobe is located in the vicinity of the angular gyrus. In addition, the hubs for the retrosplenial area (9) and the hippocampus (4) are located mesially. The hubs are presented on a standard glass brain. Furthermore, the connections of the identified hubs are indicated as lines placed between the hubs. The image is shown in radiological convention, which means that the left side of the image corresponds to the right side of the brain and vice versa.

Table 3. Hubs for which differences between coloured-hearing synaesthetes and non-synaesthetes were hypothesized with respect to the degree measure. Listed are *t*- and *p*-values obtained for the *t*-tests comparing the synaesthetes and non-synaesthetes. In addition, the effect size Cohen's *d* is indicated. Please note that only between-group differences are depicted surpassing the thresholds of a $p < .05$ and an effect size of $d > .08$. For each region, we also included the MNI coordinates of the maxima for the current densities identified with the sLORETA analysis

| Frequency band | Region | <i>t</i> <i>df</i> (23) | <i>p</i> | Cohen's <i>d</i> |
|----------------|---|----------------------------|----------|---------------------|
| Theta | Parietal cortex (l) ($X = -20, Y = -65, Z = 50$) | 2.15 | .041 | 0.879 |
| Alpha 1 | Parietal cortex (l) ($X = -20, Y = -65, Z = 50$) | 2.16 | .041 | 1.883 |
| Alpha2 | Parietal cortex (l) ($X = -20, Y = -65, Z = 50$) | 2.77 | .011 | 1.132 |
| Beta | Auditory cortex (r) ($X = 45, Y = -30, Z = 10$) | 2.37 | .026 | 0.969 |

Identification of hub regions

Hub regions for which the *degree* measure revealed differences between synaesthetes and non-synaesthetes in the some of the hypothesized regions (or hubs). There were also between-group differences in hubs for which no *a priori* hypothesis have been formulated. All between-group differences are graphically depicted in Figure 1. However, the hubs for which we have formulated *a priori* hypothesis are specifically marked in Figure 1 (black rectangles) and separately depicted in Table 3. In Table 4, the between-group differences are shown for which no *a priori* hypotheses have been formulated. The degree measures for the left-sided parietal lobe turned out to strongly differ between both

Table 4. Hubs for which differences between colored-hearing synaesthetes and non-synaesthetes were not hypothesized with respect to the degree measure

| Frequency band | Region | <i>t</i> <i>df</i> (23) | <i>p</i> | Cohen's <i>d</i> |
|----------------|---|----------------------------|----------|---------------------|
| Theta | Inferior frontal gyrus (l) ($X = -50, Y = 10, Z = 15$) | 2.08 | .048 | 0.852 |
| | Visual cortex (r) ($X = 15, Y = -85, Z = 0$) | 2.68 | .013 | 1.095 |
| Alpha 1 | Hippocampus (l) ($X = -20, Y = -10, Z = -25$) | 2.07 | .048 | 0.848 |
| | Retrosplenial area (r) ($X = 10, Y = -50, Z = 35$) | 3.33 | .003 | 1.359 |
| Alpha2 | Ventrolateral prefrontal cortex (l) ($X = -45, Y = 35, Z = 20$) | 2.92 | .007 | 1.194 |
| Beta | Angular gyrus (l) ($X = -45, Y = -65, Z = 25$) | 2.29 | .031 | 0.936 |
| | Subcentral area (r) ($X = 60, Y = -10, Z = 15$) | 2.29 | .031 | 0.936 |
| | Parietal cortex (l) Postcentral gyrus ($X = 55, Y = -25, Z = 50$) | 2.66 | .013 | 1.087 |

groups for nearly all frequency bands. With respect to the alpha2 rhythm, the right-sided auditory cortex demonstrated a stronger degree for coloured-hearing synaesthetes.

There were additional between-groups differences for the degree measure in several brain areas: left-sided inferior frontal cortex and extrastriate cortex (theta rhythm), left-sided hippocampus and the retrosplenial cortex (alpha1 rhythm), left-sided ventrolateral prefrontal cortex (alpha2 rhythm), and the left-sided inferior angular gyrus and the right-sided subcentral region (beta rhythm). There were also two additional hubs in the parietal lobe, which were different from the hubs found for the other frequency band. One hub was located within the postcentral gyrus, while the other is located in the angular gyrus (see also Figure 1).

Discussion

This study has examined the functional network characteristics of coloured-hearing synaesthetes. We were particularly interested in examining whether these synaesthetes demonstrate specific network characteristics in the parietal cortex, the auditory cortex, and the fusiform gyrus. According to recent studies and theoretical accounts, the parietal cortex is thought to play a special role in binding together the two synaesthetic perceptions (*hyperbinding*). While recent studies have used structural and functional measures during synaesthetic perceptions, in order to ascertain whether this area is specific in synaesthetes (see introduction), our research team followed a different route. We focused on the so-called resting EEG and its relation to synaesthesia. Based on resting EEG and *small-world* network analysis, we examined whether the parietal lobe, the auditory cortex, and the fusiform gyrus demonstrate functional network characteristics; thereby, supporting the notion that these areas are strongly interconnected with adjacent and distant brain structures in coloured-hearing synaesthetes. To examine the interconnectedness of these hubs, we calculated a particular measure (*degree*) as an index of how strongly these brain areas are interconnected within the *small-world* network.

Although there was no general difference between synaesthetes and non-synaesthetes in terms of the global *small-world* network parameters (number of edges, clustering coefficient, path length), the left-sided parietal lobe proved to be a strong hub in coloured-hearing synaesthetes displaying stronger *degree* measures in synaesthetes. This is particularly intriguing since this brain area demonstrates stronger degree measures for synaesthetes for nearly all frequency bands (theta, alpha1, alpha2). The location of the parietal hub for the beta band is anteriorly located in the vicinity of the postcentral gyrus. We also identified a hub in the inferior parietal lobule (particularly in the angular gyrus). These areas were not included in our *a priori* hypothesis. Therefore, we will discuss their possible role in synaesthesia in an upcoming section. Nevertheless, the vast majority of parietal hubs are located at overlapping locations. Thus, we are confident that our *a priori* hypothesis concerning the parietal lobe receives strong support; our analysis substantiates the specific role of this region for synaesthesia. A further area that we hypothesized to show stronger degree measures in synaesthesia was the auditory cortex (on the right-hand side). However, this was only demonstrated for the alpha2 band. There was no between-groups difference in the colour areas; therefore, our *a priori* hypothesis was not confirmed, at least regarding the colour areas.

In addition, several other hubs for which we did not formulate specific hypotheses were identified with stronger degree measures in synaesthetes. These hubs were found in brain areas known to be involved in controlling memory processes (alpha1: hippocampus), executive functions (alpha1 and alpha2: ventrolateral prefrontal cortex;

theta: inferior frontal cortex), the generation of perceptions (theta: extrastriate cortex; beta: subcentral area), or the generation of emotion, memory, and self-referential processing (retrosplenial area). Before we discuss these findings in the context of the literature on synaesthesia, we will first address our use of EEG and small-world network analyses for this study, since this kind of network analysis is relatively new.

Intra-cerebral sources of resting EEG

Based on the different frequency bands of the resting state EEG, we estimated the intra-cerebral sources by using sLORETA (Pascual-Marqui, 2002). These measures (current densities) were employed for our *small-world* analysis. Thus, our analysis strongly depends on the validity of sLORETA (and similar methods) to estimate intra-cerebral activation sources on the basis of EEG data. This method of estimating the intra-cerebral sources of electrical activity obtained on the scalp has been used and validated in many studies that incorporated fMRI or positron emission tomography (PET) techniques (Eryilmaz, Duru, Parlak, Ademoglu, & Demiralp, 2007; Gamma *et al.*, 2004; Meyer *et al.*, 2006; Mulert *et al.*, 2004, 2005; Tsuno *et al.*, 2002; Wieser *et al.*, 2010). We estimated the intra-cerebral sources on the basis of the resting EEG, which has been shown to be a valid biological marker for individual brain activity (Anokhin, Müller, Lindenberger, Heath, & Myers, 2006; Näpflin *et al.*, 2007). Since it is current consensus that synaesthesia is strongly determined by genetic factors (Ward & Mattingley, 2006; Ward & Simner, 2005 but see also Barnett *et al.*, 2008), it is plausible to hypothesize that the functional network, or at least parts of it, is different in synaesthetes. Graph-theoretical analysis has recently been utilized, in order to describe functional and anatomical networks in healthy subjects, as well as in patients suffering from neurological and psychiatric diseases (Bullmore & Sporns, 2009; de Haan *et al.*, 2009; Smit, Stam, Posthuma, Boomsma, & de Geus, 2008; van Dellen *et al.*, 2009). Thus, inter-individual differences have been shown to be associated with different network characteristics.

The parietal hub

Identification of a strong functional hub for all frequency bands in the synaesthetes' parietal lobe (mainly superior but with a substantial overlap with the intraparietal sulcus region) is consistent with the notion that the parietal lobe plays a specific role in binding together different perceptions. The strength, spontaneity, and robustness of synaesthetic experience has led to the view that this binding process is stronger in synaesthetes than in non-synaesthetes (*hyperbinding*), and that it is associated with particular anatomical and neurophysiological features (Hubbard, 2007; Jäncke, Beeli, Eulig, & Hanggi, 2009; Weiss & Fink, 2009). The parietal lobe serves as a strong hub, even during the resting state; thus, suggesting a specific functional (and possibly anatomical) predetermination of the synaesthetes' brain network. Hence, our finding is in line with previous studies that have specifically examined this brain region. For example, transcranial magnetic stimulation (TMS) studies suggest that this region plays a specific role in synaesthesia (Esterman *et al.*, 2006; Muggleton *et al.*, 2007). Specific anatomical features have been identified for this region, such as increased grey matter density (Rouw & Scholte, 2010; Weiss & Fink, 2009) and increased FA (2007). In addition, increased neurophysiological activation has been shown during synaesthesia in this region when applying PET, fMRI, and electrical tomography techniques (Beeli *et al.*, 2008; Grossenbacher & Lovelace, 2001; Paulesu *et al.*, 1995; Steven, Hansen, & Blakemore, 2006). In a recent study, Rouw and Scholte (Rouw & Scholte, 2010) identified increased hemodynamic responses in

the vicinity of the intraparietal sulcus, a brain area that separates the superior from the inferior parietal lobule. Taken together, our approach using resting state EEG strengthens the notion that the parietal cortex plays a pivotal role in synaesthesia and that this area is functionally and anatomically specific for this particular group.

In contrast to the other frequency bands, we identified two hubs in the parietal lobe for the beta band: one more anteriorly located in the vicinity of the postcentral gyrus and the other located in the angular gyrus. Why these hubs for the beta band are found at different locations in the parietal lobe than the parietal hubs for the other frequency band is currently unclear. However, in a very recent study with grapheme-colour synaesthetes, TMS stimulation over a left-sided parietooccipital area suppressed implicit bidirectionality in synaesthesia (Rothen *et al.*, 2010). In other words, the bidirectional cross-activation of grapheme and colour information was not possible anymore after disrupting the activity in the parietooccipital area. Since TMS stimulation to parietooccipital areas definitively coactivates the angular gyrus, it is possible that the angular gyrus is also involved in controlling bidirectionality. Accordingly, inferior parietal areas (including the angular gyrus) are also involved in synaesthesia. Our original hypothesis placed more attention on the particular location, which has been outlined by Hubbard (2007), and which is located in the vicinity of the intraparietal sulcus, not in the angular gyrus or the postcentral gyrus. Perhaps the more inferiorly located parietal hub in the angular gyrus is not involved in hyperbinding but in controlling bidirectionality. However, bidirectionality has only recently become an issue in synaesthesia. It is conceivable that the two-stage model should be transformed into a three-stage model that includes the control of bidirectionality. Whether this holds true has to be demonstrated in future studies.

The auditory hub

We also hypothesized stronger degree measures for synaesthetes in the auditory cortex and the fusiform area. We only identified stronger degree measures for coloured-hearing synaesthetes in the right-sided auditory cortex but not in the fusiform area. The between-groups difference in the auditory cortex was identified for one frequency band (alpha2). Thus, our *a priori* hypothesis did not receive strong support. However, the larger degree measure for the alpha2 band related to the resting activity in the auditory cortex and could indicate a stronger functional coupling of this area to adjacent brain areas for the colour-hearing synaesthetes. A stronger anatomical connectivity within the auditory cortex has recently been shown for an extraordinary auditory-visual synaesthete; thereby, suggesting specific anatomical features within the auditory system (Hanggi *et al.*, 2008). Furthermore, two ERP studies have shown reduced N1 amplitudes and latencies to auditory stimuli in coloured-hearing synaesthetes; thus, indicating that the auditory cortex processes auditory information at an early processing stage differently in these synaesthetes (Beeli *et al.*, 2008; Goller, Otten, & Ward., 2009). Based on monkey single-cell recording data, Goller *et al.* (2009) argue that this difference could be due to more or stronger reacting audiovisual neurons within the auditory cortex responding to visual stimuli. This is an interesting argument that should be followed-up with further experiments. Why only the right-sided auditory cortex turned out to be a strong hub in coloured-hearing synaesthetes is not entirely clear. The right-sided auditory cortex is more strongly involved in processing pitch information (Hickok & Poeppel, 2007). Thus, it is possible that tone processing in coloured-hearing synaesthetes is indeed supported by this strong hub, which is located in the right-sided auditory cortex. Future studies, nevertheless, have yet to examine whether this is true. Our findings provide support for the idea that the auditory cortex is differently organized in auditory-visual synaesthetes, even in the resting state.

Further hubs for which no *a priori* hypotheses exist

Other than the strong parietal hub that is identified for all frequency bands and the hub in the auditory cortex, we identified further hubs for different frequency bands in synaesthetes. In the section, that follows, we will shortly discuss these hubs, but we explicitly note that we did not formulate *a priori* hypothesis for these brain regions because their involvement in synaesthesia is not currently as established as the brain areas for which we have formulated our *a priori* hypotheses. Recent experiments have yet to demonstrate whether the proposed explanations hold true. These hubs were found in brain areas known to be involved in controlling memory processes (alpha1: hippocampus); executive control (alpha1 and alpha2: ventrolateral prefrontal cortex; theta: inferior frontal cortex); emotion control, memory, and self-referential processing (alpha1); sensorimotor processing (beta: postcentral gyrus); and the generation of perceptions (theta: extrastriate cortex; alpha2: beta: subcentral area). In summary, the identified hubs that overlap with brain regions in which specific anatomical and neurophysiological features have already been identified in synaesthetes. For example, previous studies have found brain activations and specific anatomical features in prefrontal regions during synaesthesia (Aleman, Rutten, Sitskoorn, Dautzenberg, & Ramsey, 2001; Beeli *et al.*, 2008; Nunn *et al.*, 2002; Paulesu *et al.*, 1995; Rouw & Scholte, 2010; Schiltz *et al.*, 1999; Sperling, Prvulovic, Linden, Singer, & Stirn, 2006; Weiss *et al.*, 2005). It has been argued that the prefrontal regions interact with modality-specific brain regions (e.g., visual, auditory, or gustatory brain areas controlling perceptual experience). This interaction might occur by associating perceptual experience with memory information or by managing memory retrieval.

A further possibility is that the frontal areas are involved in controlling conscious perception (Del Cul, Dehaene, Reyes, Bravo, & Slachevsky, 2009; Kleinschmidt, Buchel, Zeki, & Frackowiak, 1998) or in the operation of cognitive control during synaesthetic experience (Ridderinkhof, van den Wildenberg, Segalowitz, & Carter, 2004). Synaesthetic experience might interfere with 'real' experience that needs prefrontal control to manage the different and partly interfering experiences. The sensory areas (extrastriate cortex, and the subcentral area) in which hubs were localized are brain areas that are partially interconnected with regions underlying synaesthetic experience. In this study, we examined coloured-hearing synaesthetes, meaning that the visual and auditory areas are involved in generating this experience. Specific anatomical features in these areas have been shown for synaesthetes in terms of either changed grey matter densities (Hanggi, Beeli, Oechslin, & Jäncke, 2008; Jäncke *et al.*, 2009; Weiss & Fink, 2009), or changed FA measures (Rouw & Scholte, 2007). Previous studies have demonstrated that these areas are differentially activated during synaesthesia (Beeli *et al.*, 2008; Hubbard & Ramachandran, 2005; Paulesu *et al.*, 1995; Rich *et al.*, 2006; Sperling *et al.*, 2006). Further hubs were identified in the hippocampus and retrosplenial area. The hippocampus is associated with increased grey and white matter density in synaesthetes (Jäncke *et al.*, 2009; Rouw & Scholte, 2010) and with activation in this area during synaesthesia (Gray *et al.*, 2006). These findings depend on whether the examined synaesthetes are associators or projectors, with only the former showing these characteristics in the hippocampus. The hippocampus and the retrosplenial area are known to be involved in the encoding and retrieval of episodic, semantic, and spatial information (Northoff *et al.*, 2006; Piefke, Weiss, Zilles, Markowitsch, & Fink, 2003). Thus, it is conceivable that synaesthetes rely more on memory systems than non-synaesthetes (with associators showing the strongest hippocampal involvement).

The frequency bands

Most hubs were identified for the alpha band (alpha1 and alpha2). In general, alpha power and brain activity are inversely related (i.e., an increase in alpha power indicates a decrease in brain activity) (Laufs *et al.*, 2003a). The power of the alpha rhythm within a particular brain area has been shown to be directly associated with the functions controlled by these areas. For example, alpha rhythm in parietooccipital areas is modulated by attentional factors and vigilance, while the alpha rhythm within the auditory cortex (the so-called tau rhythm) varies as a function of auditory stimulation (Hari & Salmelin, 1997; Hari, Salmelin, Makela, Salenius, & Helle, 1997). Finally, alpha rhythms are broadly linked with perceptual processing and memory tasks (Klimesch, 1999; Klimesch, Freunberger, & Sauseng, 2010; Rihs, Michel, & Thut, 2009; Thut, Nietzel, Brandt, & Pascual-Leone, 2006), as well as being specifically linked with hippocampal activity during memory tasks (Babiloni *et al.*, 2009). Theta rhythms in the extrastriate areas have been identified in association with short-term maintenance of visual information in monkeys (Lee, Simpson, Logothetis, & Rainer, 2005). Beta rhythms have been observed in normal subjects during states of higher arousal, such as induced anxiety (Isotani *et al.*, 2001), but also during imagination, preparation, or observation of motor actions; thus, the beta rhythm, especially when it reflects activations of the premotor, motor, or sensorimotor system, is thought to represent the activation of the mirror neuron system (Hari 2006; Pineda, 2005). The origin of spontaneous resting beta rhythm is not well understood, although it appears to be modulated by the GABA-ergic system (Jensen *et al.*, 2005). Taken together, the EEG rhythms associated with the hub regions of the coloured-hearing synaesthetes indicate neural processes that are known to be involved in controlling particular psychological functions (perception, memory, executive control, as well as sensorimotor control) and have been previously associated with synaesthesia.

Limitations of the study

Several limitations of this study should be addressed. First, we were not able to discriminate between associators and projectors. This would have been very helpful since recent studies have demonstrated that both synaesthesia subtypes differ strongly in terms of anatomical features and brain activation (Rouw & Scholte, 2007, 2010). In future studies, we plan to disentangle possible different resting state EEG patterns for associators and projectors. Second, the relatively low number of electrodes used for this study needs to be considered because the precision of estimation of intra-cerebral sources strongly depends on the number of electrodes (Lantz, Spinelli, Menendez, Seeck, & Michel, 2001; Michel *et al.*, 2004). Although several studies have demonstrated that the precision of estimated intra-cerebral sources based on 32 channels (as used in our study) is fairly good and at least roughly corresponds with fMRI results (Mulert *et al.*, 2004), caution is warranted when making strong arguments about the exact localization of the identified hubs.

However, we would like to emphasize that James and colleagues reliably identified hippocampal activity during memory tasks (James, Britz, Vuilleumier, Hauert, & Michel, 2008; James, Morand, Barcellona-Lehmann, Michel, & Schnider, 2009). In addition, Lantz *et al.* (2001) even demonstrated that hippocampal foci of epileptic seizures can be detected even with 31 electrodes relatively precisely with a spatial error of approximately 2 cm. A further set of evidence has been added by Zumsteg and colleagues using PET simultaneously with EEG-based LORETA solutions (Zumsteg, Friedman, Wennberg, &

Wieser, 2005; Zumsteg, Friedman, Wieser, & Wennberg, 2006; Zumsteg, Wennberg, Treyer, Buck, & Wieser, 2005). They have demonstrated that LORETA is quite precise in detecting mesiotemporal foci of epileptic features.

Third, we only examined coloured-hearing synaesthetes; it has to be examined whether these findings could be replicated in other synaesthetes. Fourth, our study was based on the so-called two-stage model proposed by Hubbard (2005, 2007). Nevertheless, there is at least one additional theoretical account to explain synaesthesia. In the context of this account, synaesthesia is explained as a consequence of disinhibited feedback from higher associative areas of the cortex to lower perceptual and sensory areas (Grossenbacher & Lovelace, 2001). Whether a possible disinhibition is linked to stronger hubs in parietal and frontal areas has to be shown.

Conclusions

This paper contributes to the current literature regarding the neural underpinnings of synaesthetes in three ways. First, the study corroborates the notion that synaesthesia is related to specific network characteristics of the human brain. The underlying network comprises brain regions involved in controlling perceptions, memory processes, and executive functions. Second, it supports and extends the hypothesis that the parietal lobe plays a specific role in synaesthesia. Finally, the novelty of this study is the finding that synaesthesia is related to specific functional network characteristics, which can be measured using EEG during the rest state. Thus, there is a form of predetermination of the synaesthete's functional network even during rest, which might prepare the synaesthete to generate a particular synaesthesia in response to an appropriate inducer stimulus. This would imply that even during rest the synaesthete's brain is in a different operating mode.

Acknowledgement

We would like to thank Dr. Gian Beeli for his diligent work in collecting the data. The current work is based on a dataset that has been acquired in the context of a previous study, which has already been published (Beeli *et al.*, 2008). However, the analysis presented here is based on EEG data obtained in the resting conditions. These EEG data have not been used in the previous paper. In addition, the current manuscript uses a different theoretical and methodological approach, which allows it to reach conclusions beyond what has previously been published. In addition, we thank Drs. Juergen Haenggi and Roberto Pascual-Marqui for insightful and helpful discussion about synaesthesia, EEG analysis, and graph-theoretical data analysis. We also thank Marcus Cheetham for helpful comments on an earlier draft of this paper. The study and the writing of the paper was supported by a grant of the Swiss National Science Foundation (SNF) to L.J. (SNF 32003B_121927).

References

- Aleman, A., Rutten, G. J., Sitskoorn, M. M., Dautzenberg, G., & Ramsey, N. F. (2001). Activation of striate cortex in the absence of visual stimulation: An fMRI study of synesthesia. *Neuroreport*, *12*(13), 2827–2830. doi:10.1097/00001756-200109170-00015
- Ambrosius, U., Lietzenmaier, S., Wehrle, R., Wichniak, A., Kalus, S., Winkelmann, J., . . . Friess, E. (2008). Heritability of sleep electroencephalogram. *Biological Psychiatry*, *64*(4), 344–348. doi:10.1016/j.biopsych.2008.03.002
- Anokhin, A. P., Lutzenberger, W., & Birbaumer, N. (1999). Spatiotemporal organization of brain dynamics and intelligence: An EEG study in adolescents. *International Journal of Psychophysiology*, *33*(3), 259–273. doi:10.1016/S0167-8760(99)00064-1

- Anokhin, A. P., Müller, V., Lindenberger, U., Heath, A. C., & Myers, E. (2006). Genetic influences on dynamic complexity of brain oscillations. *Neuroscience Letters*, *397*(1–2), 93–98. doi:10.1016/j.neulet.2005.12.025
- Babiloni, C., Binetti, G., Cassetta, E., Cerboneschi, D., Dal Forno, G., Del Percio, C., *et al.* (2004). Mapping distributed sources of cortical rhythms in mild Alzheimer's disease. A multicentric EEG study. *Neuroimage*, *22*(1), 57–67. doi:10.1016/j.neuroimage.2008.08.005
- Babiloni, C., Frisoni, G. B., Pievani, M., Vecchio, F., Lizio, R., Buttiglione, M., *et al.* (2009). Hippocampal volume and cortical sources of EEG alpha rhythms in mild cognitive impairment and Alzheimer disease. *Neuroimage*, *44*(1), 123–135. doi:10.1016/j.neuroimage.2008.08.005
- Banissy, M. J., & Ward, J. (2007). Mirror-touch synesthesia is linked with empathy. *Nature Neuroscience*, *10*(7), 815–816. doi:10.1038/nn1926
- Barnett, K. J., Finucane, C., Asher, J. E., Bargary, G., Corvin, A. P., Newell, F. N., Mitchell, K. J. (2008). Familial patterns and the origins of individual differences in synaesthesia. *Cognition*, *106*, 871–893. doi:10.1016/j.cognition.2007.05.003
- Bartolomei, F., Bosma, I., Klein, M., Baayen, J. C., Reijneveld, J. C., Postma, T. J., *et al.* (2006). Disturbed functional connectivity in brain tumour patients: Evaluation by graph analysis of synchronization matrices. *Clinical Neurophysiology*, *117*(9), 2039–2049. doi:10.1016/j.clinph.2006.05.018
- Beauchamp, M. S., & Ro, T. (2008). Neural substrates of sound-touch synesthesia after a thalamic lesion. *Journal of Neuroscience*, *28*, 13696–13702. doi:10.1523/JNEUROSCI.3872-08.2008
- Beeli, G., Esslen, M., & Jäncke, L. (2005). Synaesthesia: when coloured sounds taste sweet. *Nature*, *434*(7029), 38. doi:10.1038/434038a
- Beeli, G., Esslen, M., & Jäncke, L. (2007). Frequency correlates in grapheme-color synaesthesia. *Psychological Science*, *18*, 788–792. doi:10.1111/j.1467-9280.2007.01980.x
- Beeli, G., Esslen, M., & Jäncke, L. (2008). Time course of neural activity correlated with colored-hearing synesthesia. *Cerebral Cortex*, *18*(2), 379–385. doi:10.1093/cercor/bhm072
- Brang, D., Edwards, L., Ramachandran, V. S., & Coulson, S. (2008). Is the sky 2? Contextual priming in grapheme-color synaesthesia. *Psychological Science*, *19*(5), 421–428. doi:10.1111/j.1467-9280.2008.02103.x
- Brang, D., Kanai, S., Ramachandran, V. S., & Coulson, S. (2010). Contextual priming in grapheme-color synaesthetes and yoked controls: 400 msec in the life of a synesthete. *Journal of Cognitive Neuroscience*. Advance online publication. doi:10.1162/jocn.2010.21486
- Brett, M., Johnsrude, I. S., & Owen, A. M. (2002). The problem of functional localization in the human brain. *Nature Reviews Neuroscience*, *3*(3), 243–249. doi:10.1038/nrn756
- Bullmore, E., & Sporns, O. (2009). Complex brain networks: Graph theoretical analysis of structural and functional systems. *Nature Reviews Neuroscience*, *10*(3), 186–198. doi:10.1038/nrn2575
- Cohen, J. (1969). *Statistical power analysis for the behavioral sciences*. New York: Academic Press.
- Cohen Kadosh, R., Cohen Kadosh, K., & Henik, A. (2007). The neuronal correlate of bidirectional synesthesia: A combined event-related potential and functional magnetic resonance imaging study. *Journal of Cognitive Neuroscience*, *19*(12), 2050–2059. doi:10.1162/jocn.2007.19.12.2050
- Cytowic, R. E., & Wood, F. B. (1982a). Synesthesia. I. A review of major theories and their brain basis. *Brain and Cognition*, *1*(1), 23–35. doi:10.1016/0278-2626(82)90004-5
- Cytowic, R. E., & Wood, F. B. (1982b). Synesthesia. II. Psychophysical relations in the synesthesia of geometrically shaped taste and colored hearing. *Brain and Cognition*, *1*(1), 36–49. doi:10.1016/0278-2626(82)90005-7
- de Haan, W., Pijnenburg, Y. A., Strijers, R. L., van der Made, Y., van der Flier, W. M., Scheltens, P., *et al.* (2009). Functional neural network analysis in frontotemporal dementia and Alzheimer's disease using EEG and graph theory. *BMC Neuroscience*, *10*, 101–113. doi:10.1186/1471-2202-10-101
- Del Cul, A., Dehaene, S., Reyes, P., Bravo, E., & Slachevsky, A. (2009). Causal role of prefrontal cortex in the threshold for access to consciousness. *Brain*, *132*(9), 2531–2540. doi:10.1093/brain/awp111

- De Vico Fallani, F., Maglione, A., Babiloni, F., Mattia, D., Astolfi, L., Vecchiato, G., *et al.* (2010). Cortical network analysis in patients affected by schizophrenia. *Brain Topography*, *23*(2), 214–220.
- Eryilmaz, H. H., Duru, A. D., Parlak, B., Ademoglu, A., & Demiralp, T. (2007). Neuroimaging event related brain potentials (ERP) using fMRI and dipole source reconstruction. *Conference Proceedings of the IEEE Engineering in Medicine and Biology Society, 2007*, 3384–3387. doi:10.1109/IEMBS.2007.4353057
- Esterman, M., Verstynen, T., Ivry, R. B., & Robertson, L. C. (2006). Coming unbound: Disrupting automatic integration of synesthetic color and graphemes by transcranial magnetic stimulation of the right parietal lobe. *Journal of Cognitive Neuroscience*, *18*(9), 1570–1576. doi:10.1162/jocn.2006.18.9.1570
- Freeman, L. C. (1978). Centrality in social networks: Conceptual clarification. *Social Networks*, *1*, 215–239. doi:10.1016/0378-8733(78)90021-7
- Fuchs, M., Kastner, J., Wagner, M., Hawes, S., & Ebersole, J. S. (2002). A standardized boundary element method volume conductor model. *Clinical Neurophysiology*, *113*(5), 702–712. doi:10.1016/S1388-2457(02)00030-5
- Gamma, A., Lehmann, D., Frei, E., Iwata, K., Pascual-Marqui, R. D., & Vollenweider, F. X. (2004). Comparison of simultaneously recorded [H₂(15)O]-PET and LORETA during cognitive and pharmacological activation. *Human Brain Mapping*, *22*(2), 83–96. doi:10.1002/hbm.20015
- Gianotti, L. R., Knoch, D., Faber, P. L., Lehmann, D., Pascual-Marqui, R. D., Diezi, C., *et al.* (2009). Tonic activity level in the right prefrontal cortex predicts individuals' risk taking. *Psychological Science*, *20*(1), 33–38. doi:10.1111/j.1467-9280.2008.02260.x
- Goller, A. I., Otten, L. J., & Ward, J. (2009). Seeing sounds and hearing colors: An event-related potential study of auditory-visual synesthesia. *Journal of Cognitive Neuroscience*, *21*, 1869–1881. doi:10.1162/jocn.2009.21134
- Gray, J. A., Parslow, D. M., Brammer, M. J., Chopping, S., Vythelingum, G. N., & ffytche, D. H. (2006). Evidence against functionalism from neuroimaging of the alien colour effect in synaesthesia. *Cortex*, *42*(2), 309–318. doi:10.1016/S0010-9452(08)70357-5
- Grossenbacher, P. G., & Lovelace, C. T. (2001). Mechanisms of synesthesia: Cognitive and physiological constraints. *Trends in Cognitive Sciences*, *5*(1), 36–41. doi:10.1016/S1364-6613(00)01571-0
- Hanggi, J., Beeli, G., Oechslin, M. S., & Jäncke, L. (2008). The multiple synaesthete E.S.: Neuroanatomical basis of interval-taste and tone-colour synaesthesia. *NeuroImage*, *43*(2), 192–203. doi:10.1016/j.neuroimage.2008.07.018
- Hari, R. (2006). Action-perception connection and the cortical mu rhythm. *Progress in Brain Research*, *159*, 253–260. doi:10.1016/S0079-6123(06)59017-X
- Hari, R., & Salmelin, R. (1997). Human cortical oscillations: A neuromagnetic view through the skull. *Trends in Neurosciences*, *20*(1), 44–49. doi:10.1016/S0166-2236(96)10065-5
- Hari, R., Salmelin, R., Makela, J. P., Salenius, S., & Helle, M. (1997). Magnetoencephalographic cortical rhythms. *International Journal of Psychophysiol*, *26*(1–3), 51–62. doi:10.1016/S0166-2236(96)10065-5
- Hickok, G., & Poeppel, D. (2007). The cortical organization of speech processing. *Nature Reviews Neuroscience*, *8*(5), 393–402. doi:10.1038/nrn2113
- Hubbard, E. M. (2007). Neurophysiology of synesthesia. *Current Psychiatry Reports*, *9*(3), 193–199. doi:10.1007/s11920-007-0018-6
- Hubbard, E. M., Brang, D., & Ramachandran, V. S. (2011). The Cross-Activation Theory at 10. *Journal of Neuropsychology*, *5*, 152–177. doi:10.1111/j.1748-6653.2011.02014.x
- Hubbard, E. M., & Ramachandran, V. S. (2005). Neurocognitive mechanisms of synesthesia. *Neuron*, *48*(3), 509–520. doi:10.1016/j.neuron.2005.10.012
- Humphries, M. D., & Gurney, K. (2008). Network 'small-world-ness': A quantitative method for determining canonical network equivalence. *PLoS One*, *3*(4), e0002051. doi:10.1371/journal.pone.0002051

- Humphries, M. D., Gurney, K., & Prescott, T. J. (2006). The brainstem reticular formation is a small-world, not scale-free, network. *Proceedings Biological Sciences*, *273*(1585), 503–511. doi:10.1098/rspb.2005.3354
- Isotani, T., Tanaka, H., Lehmann, D., Pascual-Marqui, R. D., Kochi, K., Saito, N., *et al.* (2001). Source localization of EEG activity during hypnotically induced anxiety and relaxation. *International Journal of Psychophysiol*, *41*(2), 143–153. doi:10.1016/S0167-8760(00)00197-5
- Ivonin, A. A., Tsitseroshin, M. N., Pogosyan, A. A., & Shuvaev, V. T. (2004). Genetic determination of neurophysiological mechanisms of cortical-subcortical integration of bioelectrical brain activity. *Neuroscience and Behavioral Physiology*, *34*(4), 369–378. doi:10.1023/B:NEAB.0000018749.36457.d9
- James, C., Morand, S., Barcellona-Lehmann, S., Michel, C. M., & Schnider, A. (2009). Neural transition from short- to long-term memory and the medial temporal lobe: A human evoked-potential study. *Hippocampus*, *19*(4), 371–378. doi:10.1002/hipo.20526
- James, C. E., Britz, J., Vuilleumier, P., Hauert, C. A., & Michel, C. M. (2008). Early neuronal responses in right limbic structures mediate harmony incongruity processing in musical experts. *Neuroimage*, *42*(4), 1597–1608. doi:10.1016/j.neuroimage.2008.06.025
- Jäncke, L., Beeli, G., Eulig, C., & Hanggi, J. (2009). The neuroanatomy of grapheme-color synesthesia. *European Journal of Neuroscience*, *29*(6), 1287–1293. doi:10.1111/j.1460-9568.2009.06673.x
- Jann, K., Dierks, T., Boesch, C., Kottlow, M., Strik, W., & Koenig, T. (2009). BOLD correlates of EEG alpha phase-locking and the fMRI default mode network. *Neuroimage*, *45*(3), 903–916. doi:10.1016/j.neuroimage.2009.01.001
- Jann, K., Koenig, T., Dierks, T., Boesch, C., & Federspiel, A. (2010). Association of individual resting state EEG alpha frequency and cerebral blood flow. *Neuroimage*, *51*(1), 365–372. doi:10.1016/j.neuroimage.2010.02.024
- Jausovec, N., & Jausovec, K. (2000). Differences in resting EEG related to ability. *Brain Topogr*, *12*(3), 229–240. doi:10.1023/A:1023446024923
- Jensen, O., Goel, P., Kopell, N., Pohja, M., Hari, R., & Ermentrout, B. (2005). On the human sensorimotor-cortex beta rhythm: Sources and modeling. *Neuroimage*, *26*(2), 347–355. doi:10.1016/j.neuroimage.2005.02.008
- Jurcak, V., Tsuzuki, D., & Dan, I. (2007). 10/20, 10/10, and 10/5 systems revisited: Their validity as relative head-surface-based positioning systems. *Neuroimage*, *34*(4), 1600–1611. doi:10.1016/j.neuroimage.2006.09.024
- Kahana, M. J., Sekuler, R., Caplan, J. B., & Kirschen, M., & Madsen, J. R. (1999). Human theta oscillations exhibit task dependence during virtual maze navigation. *Nature*, *399*(6738), 781–784. doi:10.1038/21645
- Kleinschmidt, A., Buchel, C., Zeki, S., & Frackowiak, R. S. (1998). Human brain activity during spontaneously reversing perception of ambiguous figures. *Proceedings Biological Sciences*, *265*(1413), 2427–2433. doi:10.1098/rspb.1998.0594
- Klimesch, W. (1999). EEG alpha and theta oscillations reflect cognitive and memory performance: A review and analysis. *Brain Research Brain Research Reviews*, *29*(2–3), 169–195. doi:10.1016/S0165-0173(98)00056-3
- Klimesch, W., Freunberger, R., & Sauseng, P. (2010). Oscillatory mechanisms of process binding in memory. *Neuroscience and Biobehavioral Reviews*, *34*(7), 1002–1014. doi:10.1016/j.neubiorev.2009.10.004
- Krauth, J. (1988). *Distribution-free statistics. An application-oriented approach*. Amsterdam, New York, Oxford: Elsevier.
- Kubicki, S., Herrmann, W. M., Fichte, K., & Freund, G. (1979). Reflections on the topics: EEG frequency bands and regulation of vigilance. *Pharmakopsychiatr Neuropsychopharmakol*, *12*(2), 237–245. doi:10.1055/s-0028-1094615
- Lancaster, J. L., Woldorff, M. G., Parsons, L. M., Liotti, M., Freitas, E. S., Rainey, L., *et al.* (2000). Automated Talairach Atlas labels for functional brain mapping. *Human Brain Mapping*, *10*(3), 120–131.

- Langer, N., Beeli, G., & Jäncke, L. (2010). When the sun prickles your nose: An EEG study identifying neural bases of photic sneezing. *PLoS One*, *5*(2), e9208. doi:10.1371/journal.pone.0009208
- Lantz, G., Spinelli, L., Menendez, R. G., Seeck, M., & Michel, C. M. (2001). Localization of distributed sources and comparison with functional MRI. *Epileptic Disorders, Special Issue*, *45*–58.
- Laufs, H. (2008). Endogenous brain oscillations and related networks detected by surface EEG-combined fMRI. *Human Brain Mapping*, *29*(7), 762–769. doi:10.1002/hbm.20600
- Laufs, H., Kleinschmidt, A., Beyerle, A., Eger, E., Salek-Haddadi, A., Preibisch, C., *et al.* (2003a). EEG-correlated fMRI of human alpha activity. *Neuroimage*, *19*(4), 1463–1476. doi:10.1016/S1053-8119(03)00286-6
- Laufs, H., Krakow, K., Sterzer, P., Eger, E., Beyerle, A., Salek-Haddadi, A., *et al.* (2003b). Electroencephalographic signatures of attentional and cognitive default modes in spontaneous brain activity fluctuations at rest. *Proceedings of the National Academy of Sciences of the United States of America*, *100*(19), 11053–11058. doi:10.1073/pnas.1831638100
- Lee, H., Simpson, G. V., Logothetis, N. K., & Rainer, G. (2005). Phase locking of single neuron activity to theta oscillations during working memory in monkey extrastriate visual cortex. *Neuron*, *45*(1), 147–156. doi:10.1016/j.neuron.2004.12.025
- Lehmann, D., Faber, P. L., Gianotti, L. R., Kochi, K., & Pascual-Marqui, R. D. (2006). Coherence and phase locking in the scalp EEG and between LORETA model sources, and microstates as putative mechanisms of brain temporo-spatial functional organization. *Journal of Physiology Paris*, *99*(1), 29–36. doi:10.1016/j.jphysparis.2005.06.005
- Li, Y., Liu, Y., Li, J., Qin, W., Li, K., Yu, C., *et al.* (2009). Brain anatomical network and intelligence. *PLoS Computational Biology*, *5*(5), e1000395. doi:10.1371/journal.pcbi.1000395
- Linkenkaer-Hansen, K., Smit, D. J., Barkil, A., van Beijsterveldt, T. E., Brussaard, A. B., Boomsma, D. I., *et al.* (2007). Genetic contributions to long-range temporal correlations in ongoing oscillations. *Journal of Neuroscience*, *27*(50), 13882–13889. doi:10.1523/JNEUROSCI.3083-07.2007
- Mattingley, J. B. (2009). Attention, automaticity, and awareness in synesthesia. *Annals of the New York Academy of Sciences*, *1156*, 141–167. doi:10.1111/j.1749-6632.2009.04422.x
- Mazziotta, J., Toga, A., Evans, A., Fox, P., Lancaster, J., Zilles, K., *et al.* (2001). A probabilistic atlas and reference system for the human brain: International Consortium for Brain Mapping (ICBM). *Philosophical Transactions of the Royal Society B-Biological Sciences*, *356*(1412), 1293–1322. doi:10.1098/rstb.2001.0915
- Meier, B., & Rothen, N. (2007). When conditioned responses “fire back”: Bidirectional cross-activation creates learning opportunities in synesthesia. *Neuroscience*, *147*, 569–572. doi:10.1016/j.neuroscience.2007.04.008
- Meier, B., & Rothen, N. (2009). Training grapheme-colour associations produces a synaesthetic Stroop effect, but not a conditioned synaesthetic response. *Neuropsychologia*, *47*, 1208–1211. doi:10.1016/j.neuropsychologia.2009.01.009
- Meyer, M., Baumann, S., & Jäncke, L. (2006). Electrical brain imaging reveals spatio-temporal dynamics of timbre perception in humans. *Neuroimage*, *32*(4), 1510–1523. doi:10.1016/j.neuroimage.2006.04.193
- Michel, C. M., Koenig, T., Brandeis, D., Gianotti, K. R., & Wackermann, J. (2009). *Electrical Neuroimaging*. Cambridge: Cambridge University Press.
- Michel, C. M., Murray, M. M., Lantz, G., Gonzalez, S., Spinelli, L., & Grave de Peralta, R. (2004). EEG source imaging. *Clinical Neurophysiology*, *115*(10), 2195–2222. doi:10.1016/j.clinph.2004.06.001
- Micheloyannis, S., Pachou, E., Stam, C. J., Breakspear, M., Bitsios, P., Vourkas, M., *et al.* (2006). Small-world networks and disturbed functional connectivity in schizophrenia. *Schizophrenia Research*, *87*(1–3), 60–66. doi:10.1016/j.schres.2006.06.028
- Micheloyannis, S., Vourkas, M., Tsirka, V., Karakonstantaki, E., Kanatsouli, K., & Stam, C. J. (2009). The influence of ageing on complex brain networks: A graph theoretical analysis. *Human Brain Mapping*, *30*(1), 200–208. doi:10.1002/hbm.20492

- Muggleton, N., Tsakanikos, E., Walsh, V., & Ward, J. (2007). Disruption of synaesthesia following TMS of the right posterior parietal cortex. *Neuropsychologia*, *45*(7), 1582-1585. doi:10.1016/j.neuropsychologia.2006.11.021
- Mulert, C., Jager, L., Schmitt, R., Bussfeld, P., Pogarell, O., Moller, H. J., *et al.* (2004). Integration of fMRI and simultaneous EEG: Towards a comprehensive understanding of localization and time-course of brain activity in target detection. *Neuroimage*, *22*(1), 83-94. doi:10.1016/j.neuroimage.2003.10.051
- Muller, T. J., Federspiel, A., Horn, H., Lovblad, K., Lehmann, C., Dierks, T., *et al.* (2005). The neurophysiological time pattern of illusionary visual perceptual transitions: A simultaneous EEG and fMRI study. *International Journal of Psychophysiology*, *55*(3), 299-312. doi:10.1016/j.ijpsycho.2004.09.004
- Näpflin, M., Wildi, M., & Sarnthein, J. (2007). Test-retest reliability of resting EEG spectra validates a statistical signature of persons. *Clinical Neurophysiology: Official Journal of the International Federation of Clinical Neurophysiology*, *118*(11), 2519-2524. doi:10.1016/j.clinph.2007.07.022
- Northoff, G., Heinzel, A., de Greck, M., Bermanpohl, F., Dobrowolny, H., & Panksepp, J. (2006). Self-referential processing in our brain—a meta-analysis of imaging studies on the self. *Neuroimage*, *31*(1), 440-457.
- Nunn, J. A., Gregory, L. J., Brammer, M., Williams, S. C., Parslow, D. M., Morgan, M. J., *et al.* (2002). Functional magnetic resonance imaging of synesthesia: Activation of V4/V8 by spoken words. *Nature Neuroscience*, *5*(4), 371-375. doi:10.1038/nn818
- Oostenveld, R., & Praamstra, P. (2001). The five percent electrode system for high-resolution EEG and ERP measurements. *Clinical Neurophysiology*, *112*(4), 713-719. doi:10.1016/S1388-2457(00)00527-7
- Opsahl, T. (2009). *Structure and evolution of weighted networks*. (Doctoral dissertation). Queen Mary College, University of London: London.
- Opsahl, T., Colizza, V., Panzarasa, P., & Ramasco, J. J. (2008). Prominence and Control: The Weighted Rich-Club Effect. *Physical Review Letters*, *101*(16), 1-14. doi:10.1103/PhysRevLett.101.168702
- Opsahl, T., & Panzarasa, P. (2009). Clustering in weighted networks. *Social Networks*, *31*(2), 155-163. doi:10.1016/j.socnet.2009.02.002
- Orekhova, E. V., Stroganova, T. A., Posikera, I. N., & Malykh, S. B. (2003). Heritability and “environmentability” of electroencephalogram in infants: The twin study. *Psychophysiology*, *40*(5), 727-741. doi:10.1111/1469-8986.00073
- Pascual-Marqui, R. D. (2002). Standardized low-resolution brain electromagnetic tomography (sLORETA): Technical details. *Methods and Findings in Experimental and Clinical Pharmacology*, *24*(D), 5-12.
- Paulesu, E., Harrison, J., Baron-Cohen, S., Watson, J. D., Goldstein, L., Heather, J., *et al.* (1995). The physiology of coloured hearing. A PET activation study of colour-word synaesthesia. *Brain*, *118*(Pt 3), 661-676. doi:10.1093/brain/118.3.661
- Piefke, M., Weiss, P. H., Zilles, K., Markowitsch, H. J., & Fink, G. R. (2003). Differential remoteness and emotional tone modulate the neural correlates of autobiographical memory. *Brain*, *126*(Pt 3), 650-668. doi:10.1093/brain/awg064
- Pineda, J. A. (2005). The functional significance of mu rhythms: Translating “seeing” and “hearing” into “doing”. *Brain Research Brain Research Reviews*, *50*, 57-68. doi:10.1016/j.brainresrev.2005.04.005
- Ponten, S. C., Daffertshofer, A., Hillebrand, A., & Stam, C. J. (2010). The relationship between structural and functional connectivity: Graph theoretical analysis of an EEG neural mass model. *Neuroimage*, *52*(3), 985-994. doi:10.1016/j.neuroimage.2009.10.049
- Posthuma, D., Neale, M. C., Boomsma, D. I., & de Geus, E. J. (2001). Are smarter brains running faster? Heritability of alpha peak frequency, IQ, and their interrelation. *Behavior Genetics*, *31*(6), 567-579. doi:10.1023/A:1013345411774

- Rich, A. N., Williams, M. A., Puce, A., Syngieniotis, A., Howard, M. A., McGlone, F., *et al.* (2006). Neural correlates of imagined and synaesthetic colours. *Neuropsychologia*, *44*(14), 2918–2925. doi:10.1016/j.neuropsychologia.2006.06.024
- Ridderinkhof, K. R., Van Den Wildenberg, W. P., Segalowitz, S. J., & Carter, C. S. (2004). Neurocognitive mechanisms of cognitive control: The role of prefrontal cortex in action selection, response inhibition, performance monitoring, and reward-based learning. *Brain Cognitive*, *56*(2), 129–140. doi:10.1016/j.bandc.2004.09.016
- Rihs, T. A., Michel, C. M., & Thut, G. (2009). A bias for posterior alpha-band power suppression versus enhancement during shifting versus maintenance of spatial attention. *Neuroimage*, *44*(1), 190–199. doi:10.1016/j.neuroimage.2008.08.022
- Rothen, N., Nyffeler, T., von Wartburg, R., Müri, R., & Meier, B. (2010). Parieto-occipital suppression eliminates implicit bidirectionality in grapheme-colour synaesthesia. *Neuropsychologia*, *48*(12), 3482–3487. doi:10.1016/j.neuropsychologia.2010.07.032
- Rouw, R., & Scholte, H. S. (2007). Increased structural connectivity in grapheme-color synesthesia. *Nature Neuroscience*, *10*(6), 792–797. doi:10.1038/nn1906
- Rouw, R., & Scholte, H. S. (2010). Neural basis of individual differences in synesthetic experiences. *Journal of Neuroscience*, *30*(18), 6205–6213. doi:10.1523/JNEUROSCI.3444-09.2010
- Rouw, R., Scholte, H. S., & Colizoli, O. (2011). Brain areas involved in synaesthesia: A review. *Journal of Neuropsychology*, *5*, 214–242. doi:10.1111/j.1748-6653.2011.02006.x
- Rubinov, M., Knock, S. A., Stam, C. J., Micheloyannis, S., Harris, A. W., Williams, L. M., *et al.* (2009). Small-world properties of nonlinear brain activity in schizophrenia. *Human Brain Mapping*, *30*(2), 403–416. doi:10.1002/hbm.20517
- Schiltz, K., Trocha, K., Wieringa, B. M., Emrich, H. M., Johannes, S., & Münte, T. F. (1999). Neurophysiological aspects of synesthetic experience. *The Journal of Neuropsychiatry and Clinical Neurosciences*, *11*(1), 58–65.
- Simner, J. (2007). Beyond perception: Synaesthesia as a psycholinguistic phenomenon. *Trends in Cognitive Sciences (Regul Ed)*, *11*(1), 23–29. doi:10.1016/j.tics.2006.10.010
- Simner, J., & Ward, J. (2006). Synaesthesia: The taste of words on the tip of the tongue. *Nature*, *444*, 438. doi:10.1038/444438a
- Simner, J., & Holenstein, E. (2007). Ordinal linguistic personification as a variant of synesthesia. *Journal of Cognitive Neuroscience*, *19*, 694–703. doi:10.1162/jocn.2007.19.4.694
- Sinai, A., & Pratt, H. (2003). High-resolution time course of hemispheric dominance revealed by low-resolution electromagnetic tomography. *Clinical Neurophysiology*, *114*(7), 1181–1188. doi:10.1016/S1388-2457(03)00087-7
- Smit, C. M., Wright, M. J., Hansell, N. K., Geffen, G. M., & Martin, N. G. (2006). Genetic variation of individual alpha frequency (IAF) and alpha power in a large adolescent twin sample. *International Journal of Psychophysiology*, *61*(2), 235–243. doi:10.1016/j.ijpsycho.2005.10.004
- Smit, D. J., Stam, C. J., Posthuma, D., Boomsma, D. I., & de Geus, E. J. (2008). Heritability of “small-world” networks in the brain: A graph theoretical analysis of resting-state EEG functional connectivity. *Human Brain Mapping*, *29*(12), 1368–1378. doi:10.1002/hbm.20468
- Sperling, J. M., Prvulovic, D., Linden, D. E., Singer, W., & Stirn, A. (2006). Neuronal correlates of colour-graphemic synaesthesia: A fMRI study. *Cortex*, *42*(2), 295–303.
- Sporns, O., Chialvo, D. R., Kaiser, M., & Hilgetag, C. C. (2004). Organization, development and function of complex brain networks. *Trends in Cognitive Sciences*, *8*(9), 418–425. doi:10.1016/j.tics.2004.07.008
- Sporns, O., Honey, C. J., & Kötter, R. (2007). Identification and classification of hubs in brain networks. *PLoS One*, *2*(10), e1049. doi:10.1371/journal.pone.0001049
- Stam, C. J. (2004). Functional connectivity patterns of human magnetoencephalographic recordings: A ‘small-world’ network? *Neuroscience Letters*, *355*(1–2), 25–28. doi:10.1016/j.neulet.2003.10.063
- Stam, C. J. (2010). Use of magnetoencephalography (MEG) to study functional brain networks in neurodegenerative disorders. *Journal of Neurological Sciences*, *289*(1–2), 128–134. doi:10.1016/j.jns.2009.08.028

- Stam, C. J., Jones, B. F., Nolte, G., Breakspear, M., & Scheltens, P. (2007). Small-world networks and functional connectivity in Alzheimer's disease. *Cerebral Cortex*, *17*(1), 92-99. doi:10.1093/cercor/bhj127
- Steven, M. S., Hansen, P. C., & Blakemore, C. (2006). Activation of color-selective areas of the visual cortex in a blind synesthete. *Cortex*, *42*(2), 304-308. doi:10.1016/S0010-9452(08)70356-3
- Tang, Y., Chorlian, D. B., Rangaswamy, M., Porjesz, B., Bauer, L., Kuperman, S., *et al.* (2007). Genetic influences on bipolar EEG power spectra. *International Journal of Psychophysiol*, *65*(1), 2-9. doi:10.1016/j.ijpsycho.2007.02.004
- Tesche, C. D., & Karhu, J. (2000). Theta oscillations index human hippocampal activation during a working memory task. *Proceedings of the National Academy of Sciences USA*, *97*(2), 919-924. doi:10.1073/pnas.97.2.919
- Thut, G., Nietzel, A., Brandt, S. A., & Pascual-Leone, A. (2006). Alpha-band electroencephalographic activity over occipital cortex indexes visuospatial attention bias and predicts visual target detection. *Journal of Neuroscience*, *26*(37), 9494-9502. doi:10.1523/JNEUROSCI.0875-06.2006
- Tsuno, N., Shigeta, M., Hyoki, K., Kinoshita, T., Ushijima, S., Faber, P. L., *et al.* (2002). Spatial organization of EEG activity from alertness to sleep stage 2 in old and younger subjects. *Journal of Sleep Research*, *11*(1), 43-51. doi:10.1046/j.1365-2869.2002.00288.x
- van Dellen, E., Douw, L., Baayen, J. C., Heimans, J. J., Ponten, S. C., Vandertop, W. P., *et al.* (2009). Long-term effects of temporal lobe epilepsy on local neural networks: A graph theoretical analysis of corticography recordings. *PLoS One*, *4*(11), e8081. doi:10.1371/journal.pone.0008081
- van den Heuvel, M. P., Stam, C. J., Kahn, R. S., & Hulshoff Pol, H. E. (2009). Efficiency of Functional Brain Networks and Intellectual Performance. *Journal of Neuroscience*, *29*(23), 7619-7624. doi:10.1523/jneurosci.1443-09.2009
- Verstraete, E., van den Heuvel, M. P., Veldink, J. H., Blanken, N., Mandl, R. C., Hulshoff Pol, H. E. & van den Berg, L. H. (2010). Motor network degeneration in amyotrophic lateral sclerosis: A structural and functional connectivity study. *PLoS One*, *5*, e13664. doi:10.1371/journal.pone.0013664
- Ward, J., & Mattingley, J. B. (2006). Synaesthesia: An overview of contemporary findings and controversies. *Cortex*, *42*(2), 129-136. doi:10.1016/S0010-9452(08)70336-8
- Ward, J., & Simner, J. (2005). Is synaesthesia an X-linked dominant trait with lethality in males? *Perception*, *34*(5), 611-623. doi:10.1068/p5250
- Watts, D. J., & Strogatz, S. H. (1998). Collective dynamics of 'small-world' networks. *Nature*, *393*(6684), 440-442. doi:10.1038/30918
- Weiss, P. H., & Fink, G. R. (2009). Grapheme-colour synaesthetes show increased grey matter volumes of parietal and fusiform cortex. *Brain*, *132*(Pt 1), 65-70. doi:10.1093/brain/awn304
- Weiss, P. H., Kalckert, A., & Fink, G. R. (2009) Priming letters by colors: Evidence for the bidirectionality of grapheme-color synesthesia. *Journal of Cognitive Neuroscience*, *21*, 2019-2026. doi:10.1162/jocn.2008.21166
- Weiss, P. H., Shah, N. J., Toni, I., Zilles, K., & Fink, G. R. (2001). Associating colours with people: A case of chromatic-lexical synaesthesia. *Cortex*, *37*, 750-753. doi:10.1016/S0010-9452(08)70631-2
- Weiss, P. H., Zilles, K., & Fink, G. R. (2005). When visual perception causes feeling: Enhanced cross-modal processing in grapheme-color synesthesia. *Neuroimage*, *28*(4), 859-868. doi:10.1016/j.neuroimage.2005.06.052
- Wieser, M., Haefeli, J., Butler, L., Jäncke, L., Riener, R., & Koeneke, S. (2010). Temporal and spatial patterns of cortical activation during assisted lower limb movement. *Experimental Brain Research*, *203*(1), 181-191. doi:10.1007/s00221-010-2223-5
- Zaehle, T., Frund, I., Schadow, J., Tharig, S., Schoenfeld, M. A., & Herrmann, C. S. (2009). Inter- and intra-individual covariations of hemodynamic and oscillatory gamma responses in the human cortex. *Frontiers in Human Neuroscience*, *3*, 8. doi:10.3389/neuro.09.008.2009

- Zumsteg, D., Friedman, A., Wennberg, R. A., & Wieser, H. G. (2005). Source localization of mesial temporal interictal epileptiform discharges: Correlation with intracranial foramen ovale electrode recordings. *Clinical Neurophysiology*, *116*(12), 2810–2818. doi:10.1016/j.clinph.2005.08.009
- Zumsteg, D., Friedman, A., Wieser, H. G., & Wennberg, R. A. (2006). Source localization of interictal epileptiform discharges: Comparison of three different techniques to improve signal to noise ratio. *Clinical Neurophysiology*, *117*(3), 562–571. doi:10.1016/j.clinph.2005.11.014
- Zumsteg, D., Wennberg, R. A., Treyer, V., Buck, A., & Wieser, H. G. (2005). H₂(15)O or ¹³NH₃ PET and electromagnetic tomography (LORETA) during partial status epilepticus. *Neurology*, *65*(10), 1657–1660. doi:10.1212/01.wnl.0000184516.32369.1a

Received 22 June 2010; revised version received 19 December 2010